

Accepted Manuscript

Flame retardancy and mechanical properties of epoxy thermosets modified with a novel DOPO-based oligomer

Peng Wang, Fusheng Yang, Liang Li, Zaisheng Cai



PII: S0141-3910(16)30105-7

DOI: [10.1016/j.polyimdegradstab.2016.04.005](https://doi.org/10.1016/j.polyimdegradstab.2016.04.005)

Reference: PDST 7930

To appear in: *Polymer Degradation and Stability*

Received Date: 17 December 2015

Revised Date: 24 March 2016

Accepted Date: 10 April 2016

Please cite this article as: Wang P, Yang F, Li L, Cai Z, Flame retardancy and mechanical properties of epoxy thermosets modified with a novel DOPO-based oligomer, *Polymer Degradation and Stability* (2016), doi: 10.1016/j.polyimdegradstab.2016.04.005.

This is a PDF file of an unedited manuscript that has been accepted for publication. As a service to our customers we are providing this early version of the manuscript. The manuscript will undergo copyediting, typesetting, and review of the resulting proof before it is published in its final form. Please note that during the production process errors may be discovered which could affect the content, and all legal disclaimers that apply to the journal pertain.

Flame retardancy and mechanical properties of epoxy thermosets modified with a novel DOPO-based oligomer¹

Peng Wang, Fusheng Yang, Liang Li, Zaisheng Cai*

College of Chemistry, Chemical Engineering and Biotechnology, Donghua University, Shanghai 201620, PR China

Abstract: A novel 9, 10-dihydro-9-oxa-10-phosphaphenanthrene 10-oxide (DOPO)-based oligomer indicated as PDAP was synthesized via the nucleophilic addition reaction between DOPO and imine obtained from the condensation reaction of terephthalaldehyde and *p*-phenylenediamine. The chemical structure of PDAP was characterized by FTIR, ¹H-NMR and ³¹P-NMR. The PDAP serving as co-curing agent of 4, 4'-diaminodiphenylmethane was employed to develop epoxy resins with highly improved flame retardancy. The thermal stabilities, flame-retardant and mechanical properties of epoxy thermosets were studied by thermogravimetric analysis (TGA), limiting oxygen index (LOI) measurement, UL-94 test, dynamic mechanical analysis (DMA) and tensile test. The flame-retardant mechanism of epoxy thermoset modified with PDAP was investigated by FTIR, Py-GC/MS, SEM and laser Raman spectroscopy. The results showed that with the incorporation of 7 wt% PDAP, the modified epoxy thermoset achieved a LOI value of 35.3% and V-0 rating in UL-94 test. Interestingly, all the modified thermosets showed blowing-out effects during UL-94 test. The flame-retardant mechanism was attributed to the quenching effect of phosphorus-containing free radicals and diluting effect of nonflammable gases in the gas phase, and the formation of phosphorus-rich char layers in the condensed phase. Furthermore, the results of DMA and tensile test revealed that the incorporation of PDAP decreased the glass transition temperature slightly, and meanwhile improved the tensile strength of epoxy thermoset.

Keywords: epoxy resin; DOPO; flame retardancy; mechanical property; blowing-out effect

*Corresponding author. Tel.: +86 21 67792609; Fax: +86 21 67792608.

E-mail address: zshcai@dhu.edu.cn (Zaisheng Cai).

1. Introduction

Epoxy resin, as one of the most prominent thermosetting polymers, possesses outstanding advantages such as low shrinkage, high tensile strength, good adhesion and insulation property, and excellent chemical corrosion resistance, which make it widely used in laminates, adhesives, surface coating materials, molding compounds, microelectronic materials, printed circuit boards and matrices for advanced fiber-reinforced composites [1]. However, just like other polymer materials, its highly flammable nature has severely restricted its further applications [2]. Therefore, it is imperative to develop flame retarded epoxy resin to broaden its applications in the fields requiring remarkable flame retardancy.

Over the past decades, halogenated compounds, either as reactive co-reactants or additives, have been widely utilized to develop epoxy resins with superior flame retardancy. Unfortunately, the use of such system is often accompanied by the release of corrosive or toxic gases during combustion, which could do harm to the environment [3, 4]. Therefore, many efforts have been dedicated to the flame-retardant modification of epoxy resins with halogen-free flame retardants such as boron- [3, 5], aluminum- [6, 7], silicon- [8, 9], phosphorus-containing compounds [10, 11] and nano-scaled fillers including clays [12, 13], layered double hydroxides [2, 14], graphene [15, 16] and MoS₂ [17]. Thereinto, the organophosphorus-based system has attracted great attention from both industrial and academic research studies owing to its low toxicity during combustion and outstanding flame-retardant efficiency.

Recently, 9, 10-dihydro-9-oxa-10-phosphaphenanthrene-10-oxide (DOPO), as a phosphorus-based flame retardant, has received notable attention due to the multiple structural diversification by functionalization [4]. The active hydrogen of DOPO can react with a variety of electron-deficient compounds containing imine [18-21], maleimide [22, 23], phosphazene [24, 25], silsesquioxane [26, 27], triazine [28, 29], triazine-trione [30, 31] and phosphate [32, 33] structures, leading to various DOPO-based derivatives. These derivatives, either as reactive hardeners or non-reactive additives incorporated into epoxy matrices, have endowed epoxy resins with improved flame retardancy due to the synergistic effect.

Amongst the aforementioned compounds, DOPO-based derivatives by covalently bonding DOPO and imine (DPI), with the secondary amine in the molecular structure, have captured

tremendous interest toward researchers. They could serve as co-curing agents for epoxy resins, which not only remarkably improve the flame retardancy due to phosphorus-nitrogen synergism, but also endow modified resins with other improved properties. Many efforts have been made on developing flame retarded epoxy resins based upon DPI. Yao et al. synthesized a series of DPIs, which noticeably improved the flame retardancy of epoxy thermoset at a low phosphorus content (1.0 wt%) [20, 21]. Xu et al. reported a highly effective flame retarded epoxy resin cured by a DPI co-curing agent, and the glass transition temperature (T_g) of modified thermoset decreased slightly compared to that of pure epoxy thermoset [18]. Notwithstanding the above researches which have proven that epoxy resin with improved flame retardancy can be achieved by DPI, the flame-retardant efficiency could be further enhanced by developing novel DPI oligomers with richer aryl group structure and higher phosphorus content. Moreover, further studies are needed to understand the flame-retardant mechanism of DPI in epoxy resin intensively.

In this work, a novel DPI oligomer indicated as PDAP was synthesized by nucleophilic addition of DOPO on the imine linkage. The as-prepared PDAP serving as co-curing agent was utilized to improve the flame retardancy of epoxy resin. The performances of the corresponding thermosets in terms of thermal stability, burning behavior have been studied by thermal gravimetric analysis (TGA), limiting oxygen index (LOI) measurement and UL-94 test. The flame-retardant mechanism of the modified epoxy thermosets was investigated by FTIR, Py-GC/MS, scanning electron microscopy (SEM) and laser Raman spectroscopy. Moreover, the mechanical properties of epoxy thermosets were evaluated by dynamic mechanical analysis (DMA) and tensile test.

2. Experimental

2.1. Materials

9, 10-dihydro-9-oxa-10-phosphaphenanthrene-10-oxide (DOPO) was kindly supplied by Jiangyin Hangfeng Technology Co., Ltd. (Jiangsu, China), and recrystallized from ethanol before use. Terephthalaldehyde, *p*-phenylenediamine, 4, 4'-diaminodiphenylmethane (DDM), ethanol and N, N-dimethylformamide (DMF) were all reagent grade and purchased from Sinopharm Chemical Reagent Co., Ltd. (Shanghai, China). Epoxy resin (DGEBA, commercial name: E-44,

with an epoxy value of 0.44 mol/100g) used herein was obtained from Nantong Xingchen Synthetic Material Co., Ltd. (Jiangsu, China).

2.2. Synthesis of PDAP

PDAP was prepared by a two-step synthetic method, as illustrated in **Scheme 1**. Firstly, the intermediate coded as PSB was synthesized by a typical condensation reaction. Specifically, terephthalaldehyde (5.36 g, 0.04 mol) dissolved in ethanol (80 mL) was added to a 250 mL three-necked round flask equipped with a magnetic stirrer and a reflux condenser. The mixture was then raised to 85 °C. Subsequently, *p*-phenylenediamine (4.32 g, 0.04 mol) dissolved in ethanol (80 mL) was added dropwise into the flask within 30 min. The solution was stirred at 85 °C for 6 h. Finally, the reaction mixture was filtered, washed with ethanol, and dried at 70 °C for 24 h in a vacuum oven. The brick-red solid (PSB) was recovered (7.95 g, yield: 96.5%). Secondly, the PDAP was synthesized through the nucleophilic addition reaction between DOPO and PSB. Specifically, a 250 mL three-necked round flask equipped with a magnetic stirrer and a reflux condenser was charged with DMF (80 mL), PSB (4.12 g) and DOPO (8.64 g, 0.04 mol). The reaction mixture was heated to 100 °C and stirred at 100 °C for 24 h. After cooling to room temperature, the reaction mixture was poured into ethanol (80 mL). Finally, the mixture was filtered, washed with ethanol thoroughly, and dried at 70 °C for 24 h in a vacuum oven. The light yellow solid (PDAP) was obtained (12.17 g, yield: 95.4%). Elemental analysis values: C, 71.34%; H, 4.56%; N, 4.70%; P, 9.17%. Calculated values for $(C_{38}H_{28}O_4N_2P_2)_n$: C, 71.47%; H, 4.42%; O, 10.02%; N, 4.39%; P, 9.70%.

2.3. Preparation of epoxy thermosets

Flame retarded epoxy thermoset (FREP) was prepared via a thermal curing reaction among DGEBA, DDM and PDAP. Briefly, PDAP and DDM were mixed at 120 °C for 30 min, then the homogenous solution was cooled to 90 °C. Subsequently, DGEBA was added into the mixture and blended at 90 °C for 10 min. After that, the reaction mixture was poured into the pre-heated PTFE molds and degassed in a vacuum oven at 100 °C for 5 min. The mixture was subsequently cured in a convection oven at 120 °C for 2 h and then post-cured at 160 °C for 2 h. Thereafter, the FREP was permitted to cool slowly to room temperature, in order to prevent cracking. According to the stoichiometric ratio of the reactive groups, the amount of NH functionalities of DDM and PDAP

were equal to the sum of epoxy groups in DGEBA. The control sample, was also prepared under similar processing conditions but without PDAP. The formulations of epoxy thermosets are listed in **Table 1**.

2.4. Characterization

All NMR spectra were performed at room temperature on a Bruker Avance Spectrometer (400 MHz) using DMSO- d_6 as a solvent. The ^{31}P -NMR spectrum was measured without proton decoupling.

Elemental analysis of carbon, hydrogen and nitrogen were carried out with an Elementar Vario EL III elemental analyzer (Elementar Analysensysteme GmbH, Germany). The phosphorus content was analyzed by an inductively coupled plasma-atomic emission spectrometer (Leeman Prodigy, USA).

Fourier transform infrared (FTIR) spectra were recorded between 400 cm^{-1} and 4000 cm^{-1} with a resolution of 4 cm^{-1} on a Varian 640-IR spectrometer (Varian, USA). Samples were mixed with KBr and pressed into pellets.

Limiting oxygen index (LOI) measurement was conducted on an oxygen index instrument (ATS FAAR, Italy) according to ASTM D2863-06 with the sheet size of $130\text{ mm}\times 6.5\text{ mm}\times 3\text{ mm}$; The vertical burning test (UL-94 test) was performed with the specimen size of $130\text{ mm}\times 12.7\text{ mm}\times 3\text{ mm}$ according to GB/T 2408-2008.

Thermogravimetric analysis (TGA) was carried out using a TG 209 F1 thermal analyzer (NETZSCH, Germany) with a heating rate of $10\text{ }^\circ\text{C}/\text{min}$ from $30\text{ }^\circ\text{C}$ to $800\text{ }^\circ\text{C}$ under an air or a nitrogen flow of $20\text{ mL}/\text{min}$. The sample of about 5.0 mg was measured in an alumina crucible.

Py-GC/MS analysis was performed using a FRONTIER PY-2020iD Pyrolyser coupled to a SHIMADZU GC-MS QP-2010 Ultra. The sample weight was about 2.0 mg , and the pyrolysis temperature was $600\text{ }^\circ\text{C}$. The carrier gas (Helium) flow ($1\text{ mL}/\text{min}$) was split in a ratio of 1:30 before being introduced into the gas chromatograph. The volatile pyrolysis products were separated on a 30 m HP DB-5MS capillary column (0.25 mm diameter, $0.25\text{ }\mu\text{m}$ film thickness). For the separation, the following heating program was used: 3 min at $40\text{ }^\circ\text{C}$, and then heated up to $300\text{ }^\circ\text{C}$ at a rate of $15\text{ }^\circ\text{C}/\text{min}$ and maintained at $300\text{ }^\circ\text{C}$ for 10 min .

Scanning electron microscopy (SEM) observation of char residue after UL-94 vertical test

was conducted using a Hitachi TM-1000 scanning electron microscope at an acceleration voltage of 20 kV with a magnification of 300 times. All samples were sputter-coated with gold prior to the observation.

Laser Raman spectroscopy measurement was obtained at room temperature using a SPEX-1403 laser Raman spectrometer (SPEX, USA) with the excitation provided in backscattering geometry by a 623 nm argon laser line.

Dynamic mechanical analysis (DMA) test was performed in the single-cantilever mode on a DMA Q800 instrument (TA, USA) from 30 °C to 230 °C at a heating rate of 10 °C/min, with a frequency of 1 Hz and an amplitude of 15 μm. The sample dimensions were 35 mm×6.5 mm×3 mm. Three measurements were conducted for each specimen.

The tensile test was measured with a H10K-S materials universal testing machine (Tinius Olsen, USA) complying with ASTM D638-08 at a constant cross-head speed of 5 mm/min. The results were averaged from eight measurements.

3. Results and discussion

3.1. Synthesis and characterization of PDAP

The synthetic route of PDAP is illustrated in **Scheme 1**. As an intermediate, PSB was first prepared by the condensation reaction between terephthalaldehyde and *p*-phenylenediamine. Then, the final product PDAP was synthesized through the nucleophilic addition reaction between DOPO and PSB. The chemical structure of PDAP was characterized by FTIR, ¹H-NMR and ³¹P-NMR.

Fig. 1 shows the FTIR spectra of DOPO, PSB and PDAP. In the spectrum of DOPO, the peak at 2434 cm⁻¹ belongs to the stretching vibration of P-H bond. As for PSB, the peaks at 1613 cm⁻¹ and 1692 cm⁻¹ correspond to stretching vibrations of C=N and C=O bonds respectively. In the case of PDAP, several absorption peaks including 3307 (N-H), 1593, 1475 (P-C_{Ar}), 1299(C-N), 1232 (P=O) and 1202, 919 (P-O-C_{Ar}) appear, while the characteristic peaks of P-H bond in DOPO and C=N bond in PSB vanish, suggesting that the PDAP has been synthesized successfully. Furthermore, in the spectrum of PDAP, the peak at 1670 cm⁻¹ is assigned to the stretching vibration of C=O bond in the terminal aldehyde group, which will be further confirmed by

¹H-NMR.

The ¹H-NMR spectra of DOPO, PSB and PDAP are described in **Fig. 2**. As to DOPO, the peak at 8.83 ppm belongs to the proton in –PH. In regard to PDAP, the peaks at 6.1 ppm to 8.6 ppm are attributed to the protons in the benzene ring. The proton signal in –NH- appears at 5.4 ppm to 6.1 ppm. The signal at 4.7 ppm to 5.4 ppm corresponds to the proton in methine connected with phosphorus, indicating that the reaction between the P-H bond in DOPO and C=N bond in PSB takes place. Additionally, the peak at 9.8 ppm is assigned to the proton in the terminal –CHO.

Fig. 3 depicts the ³¹P-NMR spectra of DOPO and PDAP. It is noteworthy that two peaks at 28.65 ppm and 31.84 ppm show up, while no peaks assigned to DOPO appear in the ³¹P-NMR spectrum of PDAP. The two peaks in the spectrum of PDAP may be ascribed to the formation of a stereoisomer with unequal phosphorus peaks, originating from the steric hindrance of the bulky and rigid DOPO pendant. Based upon the results obtained from FTIR, ¹H-NMR and ³¹P-NMR spectra, it is reasonable to believe that the PDAP has been successfully synthesized.

3.2. Thermal stabilities of epoxy thermosets

Thermogravimetric analysis (TGA) was utilized to study the thermal stabilities of epoxy thermosets. The thermogravimetric (TG), derivative thermogravimetric (DTG) curves in air and nitrogen atmosphere are shown in **Fig. 4**. Some important parameters, including the 5 wt% mass loss temperature ($T_{5\%}$), the maximum mass loss rate (V_{max}), the temperature at V_{max} (T_{max}), and the char yield at 700 °C are listed in **Table 2**.

As shown in **Fig. 4(a)**, the main thermal degradation process of pure EP in air occurs in two stages with T_{max} at 368.6 °C and 556.6 °C respectively, leaving little char residue at 700 °C. The first thermal decomposition takes place between 300 °C and 470 °C, corresponding to the thermal oxidative degradation, including scission of the isopropylidene linkage and the branching and crosslink reactions of molecular chains. The second stage appears from 470 °C to 700 °C, which is attributed to the further oxidation decomposition of char residues [34]. In regard to FREP, the thermal degradation behavior is similar to that of pure EP in air. As presented in **Table 2**, the $T_{5\%}$ value of FREP decreases with the increase of PDAP content. Specifically, the $T_{5\%}$ value decreases from 330.6 °C for EP to 314.5 °C for EP/PDAP4, and to 294.7 °C for EP/PDAP10. It is possible that the P-C bond in PDAP moiety is less thermally stable than the common C-C bond, and

moreover the steric hindrance effect induced by the bulky and rigid DOPO group in PDAP decreases the cross-linking density of thermoset [35, 36]. These two factors possibly account for a lower $T_{5\%}$ for thermosets modified with PDAP. Additionally, all FREPs reserve higher char yields at 700 °C compared to EP. This may be explained by the fact that the early degradation of PDAP moiety produces phosphorus-based acid, which reacts with the decomposing matrix by esterification and dehydration to promote the formation of char layer [4, 37].

In the nitrogen atmosphere, as shown in **Fig. 4(b)**, it is clear that the degradation processes of all epoxy thermosets differ from those in air, reflecting in a one-step thermal degradation profile. However, the PDAP incorporated into epoxy thermoset also leads to the decrease of $T_{5\%}$, and the increase of the char yield at 700 °C. For example, as shown in **Table 2**, the char yield at 700 °C for EP is only 17.5%, while that of EP/PDAP7 increases drastically to 24.0%. In addition, the incorporation of PDAP brings about a sharp decrease of V_{max} , and it decreases from 1.31%/°C for EP to 0.87%/°C for EP/PDAP10, implying that the FREP tends to form a more compact char layer during the thermal degradation, which can provide good insulation to the underlying matrix from the heat, thus resulting in a considerable decrease of V_{max} .

Based on the above analysis, it is reasonable to state that the incorporation of PDAP into the epoxy matrix promotes the formation of char layer, which can provide a thermally insulating barrier and inhibit the further decomposition of the epoxy matrix, leading to higher char yield at elevated temperatures.

3.3. Flame-retardant properties of epoxy thermosets

LOI and UL-94 tests are effective methods in evaluating flame retardancy, and have become the main criteria in the polymer industry. The results of flame retardancy measurements are presented in **Table 3**.

The LOI value of pure EP is found to be 25.3%, which increases following the increase of PDAP content in the epoxy thermoset. Specifically, the LOI value raises from 33.7% for EP/PDAP4 to 35.3% for EP/PDAP7, and to 37.7% for EP/PDAP10. In terms of UL-94 test, pure EP has no rating due to its serious burning drips and long burning times, while all FREPs extinguish spontaneously during vertical burning test. It achieves V-0 rating when the mass fraction of PDAP reaches 7 wt% in the epoxy thermoset. These results manifest that the

incorporation of PDAP can improve the flame retardancy of the epoxy thermoset efficiently.

To visibly observe the difference of flammability characteristics between EP and FREPs, a digital camera was employed to record the burning behaviors of EP and FREPs during vertical burning test. The video screenshots of EP and FREPs during combustion are presented in **Fig. 5**. It is noteworthy that EP is ignited quickly, and then burns aggressively with serious flaming drips, indicating its highly flammable nature. In contrast, all FREPs exhibit auto-extinguishable features, and moreover the average burning time of FREP decreases with the increase of PDAP content, suggesting its improved flame retardancy. Upon close inspection of video screenshots, it is of interest to note that all the flaming FREPs are seemingly blew out by the ejected pyrolytic gases from the surface of char layers. Similar phenomenon was also observed previously by Zhang et al. in epoxy resin modified with DOPO-POSS during combustion [26, 38]. This interesting phenomenon, suggested by Zhang et al., was named blowing-out effect.

3.4. Flame-retardant mechanism

It is generally accepted that the phosphorus-based flame retardant plays important role in flame inhibition in the gas phase and char enhancement in the condensed phase. Thus, to elucidate the flame-retardant mechanism, it is essential to investigate the properties of the carbonaceous layer and the volatile products during the thermal degradation of FREP.

3.4.1. Thermo-oxidative degradation behaviors of epoxy thermosets

To explore the flame-retardant mechanism of FREP in the condensed phase, the FTIR spectra at different temperatures were utilized to detect the details of the thermo-oxidative degradation behaviors of PDAP, EP and EP/PDAP7. Samples were thermally treated at a heating rate of 10 °C/min in a muffle furnace in air. The residues were collected when heated to specified temperature, mixed with KBr (the mass ration of char residue to KBr is 1:150), and characterized by FTIR.

Fig. 6 shows the FTIR spectra of PDAP at different temperatures. At 25 °C, several peaks including 1593, 1475 cm^{-1} (P-C_{Ar}), 1232 cm^{-1} (P=O), 1202, 919 cm^{-1} (P-O-C_{Ar}) and 754 cm^{-1} ($\text{C}_{\text{Ar}}\text{-H}$ deformation of *ortho*-substituted aromatic ring), assigned to the characteristic absorptions of DOPO group, are discerned. At 330 °C, the relative intensities of the absorption peaks due to DOPO group decrease, suggesting that DOPO moiety in PDAP may be partly released to the gas

phase. At 350 °C, some new peaks at 1635, 1098, 1054 and 530 cm^{-1} are observed in the spectrum, which are attributed to the characteristic absorptions of P-OH bond. Among these peaks, the peaks at 1098 and 1054 cm^{-1} correspond to the formation of two P-OH bonds, indicating the existence of phosphorus structures with two free OH groups. Besides, the peak at 1155 cm^{-1} is also detected, possibly related to $\text{R}(\text{OH})_2\text{P}=\text{O}$ group [39, 40]. These results suggest that phosphoric or phosphonic acid may be formed during the early degradation of PDAP. When the temperature increases to 450 °C, some new peaks at 905 and 510 cm^{-1} are observed. The peak at 510 cm^{-1} belongs to the bending vibration of O-P-O bond, and the peak at 905 cm^{-1} is assigned to the stretching vibration of P-O-P bond originating from the dehydration of P-OH bond, indicating the formation of polyphosphoric acid. Based on the above analysis, it is reasonable to conclude that phosphoric or phosphonic acid may be formed during the early degradation of PDAP, and then converted to polyphosphoric acid due to the further thermal degradation of PDAP.

Fig. 7(a) shows the FTIR spectra of EP at different temperatures. The FTIR spectrum at room temperature is identified by the characteristic absorptions of 3440, 2964, 2871, 1609, 1510, 1460, 1362, 1245, 1181, 1037 and 829 cm^{-1} . The relative intensities of characteristic peaks of EP decline sharply between 330 °C and 500 °C, suggesting that the main degradation takes places in this temperature range, which is in accordance with the TGA results. It is worth noting that two peaks at 1728 cm^{-1} and 1657 cm^{-1} appear at 350 °C, corresponding to the stretching vibrations of carbonyl and amide group respectively. The formation of carbonyl group results from oxidization of the secondary alcohol groups in cured resin [41], and the amide group stems from oxidation of the α amino carbon belonging to the DGEBA segments [42]. Furthermore, when the temperature is above 500 °C, the aromatic ring C=C stretching vibration at 1609, 1510 and 1460 cm^{-1} disappear, while a new broader peak at 1594 cm^{-1} appears, indicating the formation of polyaromatic carbons by crosslinking [10].

The FTIR spectra of the EP/PDAP7 at different temperatures are presented in **Fig. 7(b)**. The FTIR spectra of EP/PDAP7 between room temperature and 500 °C are similar to those of EP except for the absorption peak at 754 cm^{-1} . The peak at 754 cm^{-1} attributed to $\text{C}_{\text{Ar}}\text{-H}$ deformation vibration from the *ortho*-substituted aromatic ring derives from the DOPO group in PDAP moiety [4, 43]. The other characteristic peaks originating from the DOPO group are not identifiable in the

FTIR spectrum of EP/PDAP7, probably due to the overlapping of the absorptions of epoxy matrix. The relative intensity of the peak at 754 cm^{-1} decreases gradually when the temperature is above $330\text{ }^{\circ}\text{C}$, implying that the DOPO group may be partly released to the gas phase due to the rupture of P–C bond of PDAP moiety in EP/PDAP7.

When the temperature is above $500\text{ }^{\circ}\text{C}$, some new peaks appear in the char residue of EP/PDAP7. The peak at 1594 cm^{-1} corresponds to C=C stretching vibration of polyaromatic carbons, as mentioned above. The absorption band at 980 cm^{-1} belongs to the stretching vibration of P–O–P bond, and the broad peak at around 520 cm^{-1} is attributed to the bending vibration of O–P–O bond [44]. What is more, the peak at 1096 cm^{-1} is assigned to the stretching vibration of P–O–C_{Ar} bond [45]. In consideration of the fact that the thermo-oxidative degradation of PDAP can produce phosphoric/phosphonic acid and polyphosphoric acid, it can be deduced that these acids can react with the decomposing epoxy matrix by esterification and dehydration to promote the formation of char residues.

Based upon the results obtained above, it is reasonable to conclude that during the thermal degradation of FREP, the acids originating from the degradation of PDAP moiety react with the decomposing matrix, resulting in char layers with polyaromatic structures bridged by P–O–C and P–O–P bonds [46]. The char layers can provide a thermally insulating layer or barrier on the surface of epoxy matrix, which can reduce heat and oxygen transmission into the material, thus endowing the epoxy thermoset with improved flame retardancy in the condensed phase.

3.4.2. Pyrolysis behaviors of epoxy thermosets

To gain insight into the flame-retardant mechanism of FREP in the gas phase, the Py-GC/MS was employed to analyze the pyrolysis products of PDAP, EP and EP/PDAP7.

Fig. 8 gives the pyrogram and pyrolysis products of PDAP. The main pyrolysis products of PDAP are *p*-phenylenediamine, diphenyl, dibenzofuran, *o*-phenylphenol and fluorene. The formation of dibenzofuran, according to Balabanovich et al. [47], is ascribed to the splitting of P–C and P–O bonds of DOPO-based derivative, while a hydrolysis step followed by scission of P–C bond is attributed to the generation of *o*-phenylphenol. The formation of these pyrolysis products, especially dibenzofuran, can be regarded as a sign for production of phosphorus-containing fragments in the gas phase.

Fig. 9 shows the pyrograms of EP and EP/PDAP7, and the assigned products are collected in **Table 4**. As shown in **Table 4**, the main pyrolysis products of EP are phenol, 4-isopropylphenol, 4-isopropenylphenol, 4-(2-phenylpropan-2-yl) phenol, 2-methyl-4-(2-phenylpropan-2-yl) phenol, 4-(2-(benzofuran-5-yl) propan-2-yl) phenol and 4, 4'-methylenebis (N, N-dimethylaniline). The pyrolysis products of EP/PDAP7 are similar to those of EP, whereas the relative areas of pyrolysis products have been greatly altered. The incorporation of PDAP into epoxy thermoset induces the decomposition of the epoxy matrix, resulting in the release of larger chain segments. For example, the relative areas of products with m/z 228, 252, 240 and 254 increase from 0.47%, 3.24%, 3.67% and 2.14% for EP to 17.85%, 5.85%, 5.18% and 3.12% for EP/PDAP7 respectively. Similar results were obtained in the pyrolysis of epoxy thermosets containing DOPO [48] and DOPO-based derivative [45].

It should be noted that some volatiles including diphenyl, dibenzofuran and *o*-phenylphenol, which appear in the pyrolysis products of PDAP, recur in the pyrolysis products of EP/PDAP7, suggesting that phosphorus-containing fragments exist in the gas phase as mentioned previously. These phosphorus-containing fragments, such as PO \cdot and PO $_2\cdot$, can scavenge the H and OH free radicals in the flame, and inhibit the free radical chain reaction of combustion. Moreover, the pyrolysis products of EP/PDAP7 include nitrogen-containing compounds, which can be decomposed to nonflammable gases during combustion. The nitrogen-containing nonflammable gases combined with CO $_2$ can dilute ignitable gases and cut off the supply of oxygen, thus exerting flame-retardant effect in the gas phase. In conclusion, the flame-retardant mechanism in the gas phase is ascribed to the quenching effect of phosphorus-containing free radicals and diluting effect of nonflammable gases.

3.4.3. Morphology and structure of residual char

The digital photos of char residues after vertical burning test were recorded by a camera as shown in **Fig. 10(a)**. Pure EP shows bits of residual char with a fragmentary morphology, whereas all FREPs exhibit relatively intact char layers. Moreover, in regard to FREPs, it is of interest to note that some cracked holes are observed on the surface of char residues, which are ascribed to the ejected pyrolytic gases from the surface of char layer during combustion.

To get more details about the char residues, the micromorphology of the interior and exterior

char layers corresponding to the blue box in the digital photos were investigated by SEM as shown in **Fig. 10(b)** and **Fig. 10(c)**. Similar to the results observed in the digital photos, pure EP reveals a incompact and cracked surface, suggesting its intrinsic poor flame retardancy. In contrast, the exterior char layers of FREPs present integral, compact and intumescent structures. It is of interest to note that the interior char layers of FREPs show honeycombed cavity structures with considerable holes. This integral, compact and intumescent char layer with honeycombed cavity inside can serve as a thermal insulation layer, and accumulate pyrolytic gases containing considerable phosphorus-containing free radicals and nonflammable gases. When the amount of pyrolytic gases exceed the holding capacity of the char layer, the pyrolytic gases containing free radicals such as $\text{PO}\cdot$ and $\text{PO}_2\cdot$ and nonflammable gases like CO_2 are instantly released to blow out the flame, leaving cracked holes on the surface of char layer.

With a view to investigating the morphology of char layer produced under inert nitrogen atmosphere, the epoxy thermosets with the size of $12.7 \text{ mm} \times 12.7 \text{ mm} \times 3.0 \text{ mm}$ were heated from room temperature to $600 \text{ }^\circ\text{C}$ at a heating rate of $10 \text{ }^\circ\text{C}/\text{min}$ in a muffle furnace under nitrogen, and permitted to cool slowly to room temperature. The char residues were collected and recorded by a digital camera as shown in **Fig. 11**. Pure EP exhibits a fragmentary and collapsed char layer, which is in accordance with its inferior flame-retardant property. In sharp contrast to EP, all FREPs remain their shapes with cubic-like morphology, and present intumescent char layers. To observe the inner char layers of FREPs, the surface char layers were carefully stripped off by a needle. Surprisingly, the internal structure of residual chars for FREPs present huge cavities, which can accumulate considerable pyrolytic gases. The formation of this compact and intumescent char layer with huge cavity inside can be speculated as follows: when exposed to heat, FREP tends to form a compact and integral char layer on the surface of matrix. The pyrolytic gases originating from the thermal degradation can be accumulated in the char layer to form intumescent structure, thus leading to the formation of intumescent char layer with cavity inside.

Laser Raman spectroscopy was employed to characterize the structure and component of the char residues. Samples were thermally treated at a heating rate of $10 \text{ }^\circ\text{C}/\text{min}$ in a muffle furnace in air. The solid residues were collected when heated to $600 \text{ }^\circ\text{C}$, and characterized by Laser Raman spectroscopy as shown in **Fig. 12**. All spectra exhibit two peaks at 1360 cm^{-1} (D band) and 1593

cm^{-1} (G band), corresponding to the vibration of the carbon atoms in disordered graphite or glassy carbons and the carbon atoms in crystalline graphite respectively [49]. The degree of graphitization of the residual char can be calculated by a ratio of the integrated intensity of D and G bands (I_D/I_G). Generally, a lower I_D/I_G value means a higher graphitization degree of the resultant char [50]. The residual char with a higher graphitization degree is more conducive to restrain the diffusion of heat and mass during pyrolysis due to its higher thermal stability and compactness. As shown in **Fig. 12**, the I_D/I_G value follows the sequence of EP (2.54) > EP/PDAP4 (2.42) > EP/PDAP7 (2.37) > EP/PDAP10 (2.25), indicating that the residual chars of FREPs are more cohesive and compact compared to that of pure EP, which is in accordance with the result obtained by SEM observation. The residue with a more cohesive and compact char layer is beneficial for isolating the matrix from the heat and oxygen, thus improving the flame retardancy of epoxy thermoset.

Based upon the results obtained above, the flame-retardant mechanism of FREP is mainly ascribed to the quenching effect of free radicals and the diluting effect of nonflammable gases in the gas phase, and the formation of phosphorus-rich char layers in the condensed phase. More specifically, the phosphoric/phosphonic acid and polyphosphoric acid originating from the degradation of PDAP moiety react with decomposing epoxy matrix by esterification and dehydration, resulting in char layers with polyaromatic structures bridged by P-O-C and P-O-P bonds. The phosphorus-rich char layers can provide good insulation to the underlying matrix from the heat and oxygen, thus playing flame retarded role in the condensed phase. In the gas phase, the pyrolysis of FREP produces phosphorus-containing fragments including PO and PO_2 free radicals, and nonflammable gases such as CO_2 and nitrogen-containing nonflammable gases. The PO and PO_2 free radicals can scavenge the $\text{H}\cdot$ and $\text{OH}\cdot$ in the flame, and the nonflammable gases can dilute ignitable gases and cut off the supply of oxygen, thus exerting flame-retardant effect.

The observed blowing-out effect during vertical burning test may be explained as follows: as illustrated in **Fig. 13**, during combustion, a compact, intumescent and phosphorus-rich char layer with honeycombed cavity inside can be rapidly formed on the surface of burning matrix, which accumulates pyrolytic gases containing considerable free radicals such as $\text{PO}\cdot$ and $\text{PO}_2\cdot$, and nonflammable gases like CO_2 . When the amount of pyrolytic gases surpass the holding capacity of

the char layer, the pyrolytic gases are instantly released to blow out the flame, leaving cracked holes on the surface of char layer.

3.5. Mechanical properties of epoxy thermosets

DMA was employed to investigate the dynamic mechanical behaviors of epoxy thermosets. The storage modulus and $\tan \delta$ versus temperature plots of epoxy thermosets are shown in **Fig. 14**. The storage modulus of neat EP at the initial temperature (40 °C) is 1,931 MPa, and it raises with the increase of PDAP content and further reaches 2,397 MPa for EP/PDAP10. Similar results have also been obtained in epoxy resins modified by DOPO-based derivatives [18, 35]. The bulky and rigid DOPO units linked to the backbone of PDAP moiety increase the rigidity of the epoxy thermosets, thus leading to higher storage modulus at the initial temperature.

The glass transition temperature (T_g) is determined by the peak of $\tan \delta$ curve. As shown in **Fig. 14**, EP shows a T_g of 171 °C, and a slight decrease in T_g is observed with the incorporation of PDAP into epoxy thermoset. For example, the T_g of EP/PDAP4 is found to be 166 °C, and that of EP/PDAP7 is 163 °C. To explain this phenomenon, it should be noted that the large steric hindrance of DOPO units may elevate the activation energy of the curing reaction between curing agent and epoxy resin, which reduces the cross-linking density of epoxy thermoset [35], thus resulting in the decrease of T_g . However, the incorporation of the bulky and rigid DOPO units also inhibit the mobility of macromolecular chains, thus compensating for the decrease of cross-linking density [18, 51]. These two competing factors are responsible for a slight decrease of T_g .

To further evaluate the influence of PDAP on the mechanical properties of epoxy thermosets, the tensile strength and elongation at break of epoxy thermosets were measured. As shown in **Fig. 15**, EP shows a tensile strength of 74.16 MPa, and elongation at break of 8.20%. The incorporation of PDAP increases the tensile strength of epoxy thermoset. Specifically, the tensile strength increases from 77.32 MPa for EP/PDAP4 to 82.44 MPa for EP/PDAP7, and to 83.25 MPa for EP/PDAP10. As to the elongation at break, it reduces gradually with the increase of PDAP, from 7.71% (EP/PDAP4) to 7.36% (EP/PDAP7) and to 6.21% (EP/PDAP10). This may be attributed to the bulky and rigid DOPO units attached to the backbone of PDAP moiety, resulting in a polymer network with stronger restrictions to molecular motion.

4. Conclusions

In this work, a novel DOPO-based oligomer indicated as PDAP was synthesized through a two-step reaction, and its chemical structure was confirmed by FTIR, $^1\text{H-NMR}$, $^{31}\text{P-NMR}$. The as-prepared PDAP, serving as co-curing agent of DDM incorporated into epoxy matrix, endowed the epoxy thermoset with highly improved flame retardancy. With the incorporation of 7 wt% PDAP, the epoxy thermoset achieved a LOI value of 35.3% and V-0 rating in UL-94 test. All the modified epoxy thermosets showed blowing-out effects during UL-94 test, which were ascribed to the concentrated release of pyrolytic gases containing phosphorus-based free radicals and nonflammable gases. The flame-retardant mechanism was attributed to the quenching effect of phosphorus-containing free radicals and diluting effect of nonflammable gases in the gas phase, and the formation of phosphorus-rich char layers in the condensed phase. Furthermore, the incorporation of PDAP decreased the T_g slightly, and improved the tensile strength of epoxy thermoset.

Acknowledgements

This work was financially supported by Program for Specialized Research Fund for the Doctoral Program of Higher Education in China (Grant No. 20130075130002) and the National Natural Science Foundation of China (Grant No. 51303022 and 51203018).

References

- [1] Chruściel JJ, Leśniak E. Modification of epoxy resins with functional silanes, polysiloxanes, silsesquioxanes, silica and silicates. *Prog Polym Sci* 2015;41:67-121.
- [2] Kalali EN, Wang X, Wang DY. Functionalized layered double hydroxide-based epoxy nanocomposites with improved flame retardancy and mechanical properties. *J Mater Chem A* 2015;3(13):6819-26.
- [3] Yang HY, Wang X, Yu B, Song L, Hu Y, Yuen RKK. Effect of borates on thermal degradation and

flame retardancy of epoxy resins using polyhedral oligomeric silsesquioxane as a curing agent.

Thermochim Acta 2012;535:71-8.

[4] Carja I-D, Serbezeanu D, Vlad-Bubulac T, Hamciuc C, Coroaba A, Lisa G, et al. A straightforward, eco-friendly and cost-effective approach towards flame retardant epoxy resins. *J Mater Chem A* 2014;2(38):16230-41.

[5] Zhou Y, Feng J, Peng H, Qu HQ, Hao JW. Catalytic pyrolysis and flame retardancy of epoxy resins with solid acid boron phosphate. *Polym Degrad Stab* 2014;110:395-404.

[6] Wang JY, Qian LJ, Xu B, Xi W, Liu XX. Synthesis and characterization of aluminum poly-hexamethylenephosphinate and its flame-retardant application in epoxy resin. *Polym Degrad Stab* 2015;122:8-17.

[7] Ma JJ, Yang JX, Huang YW, Ke C. Aluminum-organophosphorus hybrid nanorods for simultaneously enhancing the flame retardancy and mechanical properties of epoxy resin. *J Mater Chem* 2012;22(5):2007-17.

[8] Raimondo M, Russo S, Guadagno L, Longo P, Chirico S, Mariconda A, et al. Effect of incorporation of POSS compounds and phosphorous hardeners on thermal and fire resistance of nanofilled aeronautic resins. *RSC Adv* 2015;5(15):10974-86.

[9] Murias P, Maciejewski H, Galina H. Epoxy resins modified with reactive low molecular weight siloxanes. *Eur Polym J* 2012;48(4):769-73.

[10] Tian NN, Gong J, Wen X, Yao K, Tang T. Synthesis and characterization of a novel organophosphorus oligomer and its application in improving flame retardancy of epoxy resin. *RSC Adv* 2014;4(34):17607-14.

[11] Chen XL, Jiao CM, Li SX, Sun J. Flame retardant epoxy resins from bisphenol-A epoxy cured

- with hyperbranched polyphosphate ester. *J Polym Res* 2011;18(6):2229-37.
- [12] Wang JJ, Feng LJ, Feng YN, Yan AJ, Ma XY. Preparation and properties of organic rectorite/epoxy resin nano-composites. *Polym Plast Technol Eng* 2012;51(15):1583-8.
- [13] Katsoulis C, Kandare E, Kandola BK. The effect of nanoparticles on structural morphology, thermal and flammability properties of two epoxy resins with different functionalities. *Polym Degrad Stab* 2011;96(4):529-40.
- [14] Li C, Wan JT, Kalali EN, Fan H, Wang DY. Synthesis and characterization of functional eugenol derivative based layered double hydroxide and its use as a nanoflame-retardant in epoxy resin. *J Mater Chem A* 2015;3(7):3471-9.
- [15] Yu B, Shi YQ, Yuan BH, Qiu SL, Xing WY, Hu WZ, et al. Enhanced thermal and flame retardant properties of flame-retardant-wrapped graphene/epoxy resin nanocomposites. *J Mater Chem A* 2015;3(15):8034-44.
- [16] Liu S, Yan HQ, Fang ZP, Wang H. Effect of graphene nanosheets on morphology, thermal stability and flame retardancy of epoxy resin. *Compos Sci Technol* 2014;90:40-7.
- [17] Feng XM, Xing WY, Song L, Hu Y. In situ synthesis of a MoS₂/CoOOH hybrid by a facile wet chemical method and the catalytic oxidation of CO in epoxy resin during decomposition. *J Mater Chem A* 2014;2(33):13299-308.
- [18] Xu WH, Wirasaputra A, Liu SM, Yuan YC, Zhao JQ. Highly effective flame retarded epoxy resin cured by DOPO-based co-curing agent. *Polym Degrad Stab* 2015;122:44-51.
- [19] Chao PJ, Li YJ, Gu XY, Han DD, Jia XQ, Wang MQ, et al. Novel phosphorus-nitrogen-silicon flame retardants and their application in cycloaliphatic epoxy systems. *Polym Chem* 2015;6(15):2977-85.

- [20] Xiao L, Sun DC, Niu TL, Yao YW. Syntheses of two DOPO-based reactive additives as flame retardants and co-curing agents for epoxy resins. *Phosphorus, Sulfur Silicon Relat Elem* 2014;189(10):1564-71.
- [21] Gu LQ, Chen GA, Yao YW. Two novel phosphorus-nitrogen-containing halogen-free flame retardants of high performance for epoxy resin. *Polym Degrad Stab* 2014;108:68-75.
- [22] Yang S, Wang J, Huo SQ, Wang M, Cheng LF. Synthesis of a phosphorus/nitrogen-containing additive with multifunctional groups and its flame-retardant effect in epoxy resin. *Ind Eng Chem Res* 2015;54(32):7777-86.
- [23] Yang S, Wang J, Huo SQ, Cheng LF, Wang M. Preparation and flame retardancy of an intumescent flame-retardant epoxy resin system constructed by multiple flame-retardant compositions containing phosphorus and nitrogen heterocycle. *Polym Degrad Stab* 2015;119:251-9.
- [24] Qian LJ, Ye LJ, Qiu Y, Qu SR. Thermal degradation behavior of the compound containing phosphaphenanthrene and phosphazene groups and its flame retardant mechanism on epoxy resin. *Polymer* 2011;52(24):5486-93.
- [25] Xu MJ, Xu GR, Leng Y, Li B. Synthesis of a novel flame retardant based on cyclotriphosphazene and DOPO groups and its application in epoxy resins. *Polym Degrad Stab* 2016;123:105-14.
- [26] Zhang WC, Li XM, Yang RJ. Novel flame retardancy effects of DOPO-POSS on epoxy resins. *Polym Degrad Stab* 2011;96(12):2167-73.
- [27] Wang Z, Wu W, Zhong YH, Ruan MZ, Hui LL. Flame-retardant materials based on phosphorus-containing polyhedral oligomeric silsesquioxane and bismaleimide/diallylbisphenol a with improved thermal resistance and dielectric properties. *J Appl Polym Sci* 2015;132(9):1-10.
- [28] Li ZQ, Yang RJ. Study of the synergistic effect of polyhedral oligomeric

octadiphenylsulfonylsilsesquioxane and 9,10-dihydro-9-oxa-10-phosphaphenanthrene-10-oxide on flame-retarded epoxy resins. *Polym Degrad Stab* 2014;109:233-9.

[29] Xiong YQ, Jiang ZJ, Xie YY, Zhang XY, Xu WJ. Development of a DOPO-containing melamine epoxy hardeners and its thermal and flame-retardant properties of cured products. *J Appl Polym Sci* 2013;127(6):4352-8.

[30] Qian LJ, Qiu Y, Sun N, Xu ML, Xu GZ, Xin F, et al. Pyrolysis route of a novel, flame retardant constructed by phosphaphenanthrene and triazine-trione groups and its flame-retardant effect on epoxy resin. *Polym Degrad Stab* 2014;107:98-105.

[31] Perret B, Schartel B, Stöß K, Ciesielski M, Diederichs J, Döring M, et al. Novel DOPO-based flame retardants in high-performance carbon fibre epoxy composites for aviation. *Eur Polym J* 2011;47(5):1081-9.

[32] Wang X, Hu Y, Song L, Xing WY, Lu HD, Lv P, et al. Flame retardancy and thermal degradation mechanism of epoxy resin composites based on a DOPO substituted organophosphorus oligomer. *Polymer* 2010;51(11):2435-45.

[33] Wang X, Hu Y, Song L, Yang HY, Xing WY, Lu HD. Synthesis and characterization of a DOPO-substituted organophosphorus oligomer and its application in flame retardant epoxy resins. *Prog Org Coat* 2011;71(1):72-82.

[34] Qian XD, Song L, Hu Y, Yuen RKK. Thermal degradation and flammability of novel organic/inorganic epoxy hybrids containing organophosphorus-modified oligosiloxane. *Thermochim Acta* 2013;552:87-97.

[35] Liu SM, Chen JB, Zhao JQ, Jiang ZJ, Yuan YC. Phosphaphenanthrene-containing borate ester as a latent hardener and flame retardant for epoxy resin. *Polym Int* 2015;64(9):1182-90.

- [36] Wu ZJ, Li JL, Chen YP, Wang Z, Li SC. Effect of 9,10-Dihydro-9-Oxa-10-Phosphaphenanthrene-10-Oxide on Liquid Oxygen Compatibility of Bisphenol A Epoxy Resin. *J Appl Polym Sci* 2014;131(19):40848.
- [37] Liang B, Cao J, Hong XD, Wang CS. Synthesis and properties of a novel phosphorous-containing flame-retardant hardener for epoxy resin. *J Appl Polym Sci* 2013;128(5):2759-65.
- [38] Zhang WC, Li XM, Yang RJ. Blowing-out effect in epoxy composites flame retarded by DOPO-POSS and its correlation with amide curing agents. *Polym Degrad Stab* 2012;97(8):1314-24.
- [39] Balabanovich AI. Thermal decomposition study of intumescent additives: Pentaerythritol phosphate and its blend with melamine phosphate. *Thermochim Acta* 2005;435(2):188-96.
- [40] Schartel B, Perret B, Dittrich B, Ciesielski M, Krämer J, Müller P, et al. Flame Retardancy of Polymers: The Role of Specific Reactions in the Condensed Phase. *Macromol Mater Eng* 2016;301(1):9-35.
- [41] Li K, Wang K, Zhan MS, Xu W. The change of thermal-mechanical properties and chemical structure of ambient cured DGEBA/TEPA under accelerated thermo-oxidative aging. *Polym Degrad Stab* 2013;98(11):2340-6.
- [42] Zahra Y, Djouani F, Fayolle B, Kuntz M, Verdu J. Thermo-oxidative aging of epoxy coating systems. *Prog Org Coat* 2014;77(2):380-7.
- [43] Perret B, Schartel B, Stöß K, Ciesielski M, Diederichs J, Döring M, et al. A new halogen-free flame retardant based on 9,10-dihydro-9-oxa-10-phosphaphenanthrene-10-oxide for epoxy resins and their carbon fiber composites for the automotive and aviation industries. *Macromol Mater Eng* 2011;296(1):14-30.
- [44] Gallo E, Schartel B, Braun U, Russo P, Acierno D. Fire retardant synergisms between nanometric

Fe₂O₃ and aluminum phosphinate in poly(butylene terephthalate). *Polym Adv Technol* 2011;22(12):2382-91.

[45] Qian LJ, Qiu Y, Wang JY, Xi W. High-performance flame retardancy by char-cage hindering and free radical quenching effects in epoxy thermosets. *Polymer* 2015;68:262-9.

[46] Zhao W, Liu JP, Peng H, Liao JY, Wang XJ. Synthesis of a novel PEPA-substituted polyphosphoramidate with high char residues and its performance as an intumescent flame retardant for epoxy resins. *Polym Degrad Stab* 2015;118:120-9.

[47] Balabanovich AI, Pospiech D, Häußler L, Harnisch C, Döring M. Pyrolysis behavior of phosphorus polyesters. *J Anal Appl Pyrolysis* 2009;86(1):99-107.

[48] Zhang WC, He XD, Song TL, Jiao QJ, Yang RJ. Comparison of intumescence mechanism and blowing-out effect in flame-retarded epoxy resins. *Polym Degrad Stab* 2015;112:43-51.

[49] Jiang SD, Bai ZM, Tang G, Song L, Stec AA, Hull TR, et al. Synthesis of Mesoporous Silica@Co-Al Layered Double Hydroxide Spheres: Layer-by-Layer Method and Their Effects on the Flame Retardancy of Epoxy Resins. *ACS Appl Mater Interfaces* 2014;6(16):14076-86.

[50] Wang D, Zhou KQ, Yang W, Xing WY, Hu Y, Gong XL. Surface Modification of Graphene with Layered Molybdenum Disulfide and Their Synergistic Reinforcement on Reducing Fire Hazards of Epoxy Resins. *Ind Eng Chem Res* 2013;52(50):17882-90.

[51] Artner J, Ciesielski M, Walter O, Döring M, Perez RM, Sandler JKW, et al. A novel DOPO-based diamine as hardener and flame retardant for epoxy resin systems. *Macromol Mater Eng* 2008;293(6):503-14.

Figure Captions

- Fig. 1.** FTIR spectra of DOPO, PSB and PDAP
- Fig. 2.** ^1H -NMR spectra of DOPO, PSB and PDAP in $\text{DMSO-}d_6$
- Fig. 3.** ^{31}P -NMR spectra of DOPO and PDAP in $\text{DMSO-}d_6$
- Fig. 4.** TG and DTG curves of epoxy thermosets in air (a) and nitrogen (b) atmosphere
- Fig. 5.** Video screenshots of epoxy thermosets during the vertical burning test
- Fig. 6.** FTIR spectra of PDAP at different temperatures
- Fig. 7.** FTIR spectra of EP (a) and EP/PDAP7 (b) at different temperatures
- Fig. 8.** Pyrogram of PDAP and corresponding pyrolysis products
- Fig. 9.** Pyrograms of EP and EP/PDAP7
- Fig. 10.** Digital photos (a) and SEM micrographs (b, c) of the char residues after vertical burning test
- Fig. 11.** Digital photos of epoxy thermosets before (a) and after (b, c) thermal degradation in nitrogen
- Fig. 12.** Raman spectra of the char residues of epoxy thermosets
- Fig. 13.** Schematic illustration for the blowing-out effect of FREP during combustion
- Fig. 14.** DMA curves of epoxy thermosets
- Fig. 15.** Tensile strength and elongation at break of epoxy thermosets

Table 1. Formulations of epoxy thermosets

Specimen	Composition (g)			PDAP (wt%)	P (wt%)
	DGEBA	DDM	PDAP		
EP	100	21.82	0	0	0
EP/PDAP4	100	20.98	5.04	4	0.37
EP/PDAP7	100	20.31	9.06	7	0.64
EP/PDAP10	100	19.60	13.29	10	0.92

Table 2. Thermal parameters of epoxy thermosets

Samples	$T_{5\%}$ (°C)		T_{max} (°C)		V_{max} (%/°C)		Char yield at 700 °C (%)	
	N ₂	Air	N ₂	Air	N ₂	Air	N ₂	Air
EP	354.7	330.6	379.9	368.6, 556.6	1.31	1.48, 0.45	17.5	0.5
EP/PDAP4	326.9	314.5	368.8	361.0, 598.5	0.96	0.83, 0.34	22.6	1.0
EP/PDAP7	315.4	303.2	364.6	356.3, 606.8	0.90	0.79, 0.32	24.0	1.2
EP/PDAP10	309.1	294.7	360.7	347.7, 615.7	0.87	0.77, 0.26	24.4	2.5

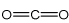
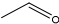
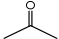
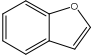
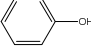
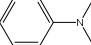
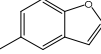
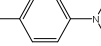


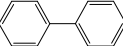
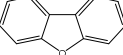
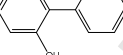
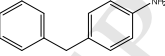
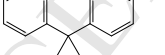
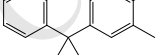
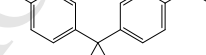
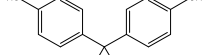
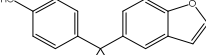

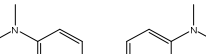
Table 3. LOI value and UL-94 rating of epoxy thermosets

Specimen	LOI (%)	UL-94, 3.0 mm bar		
		$t_1+t_2^a$ (s)	Dripping	Rating
EP	25.3	BC ^b	Yes	No rating
EP/PDAP4	33.7	5.6+8.2	No	V-1
EP/PDAP7	35.3	3.2+4.7	No	V-0
EP/PDAP10	37.7	2.1+2.9	No	V-0

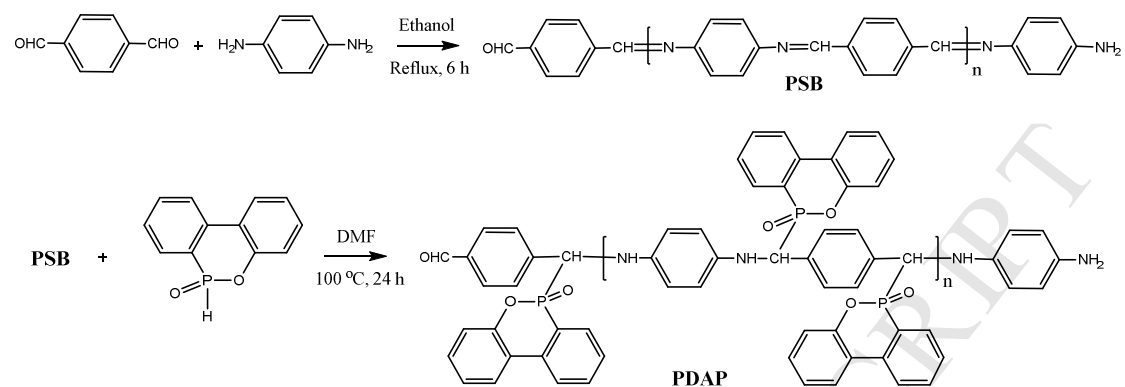
^a t_1 and t_2 , average combustion times after the first and the second applications of the flame.

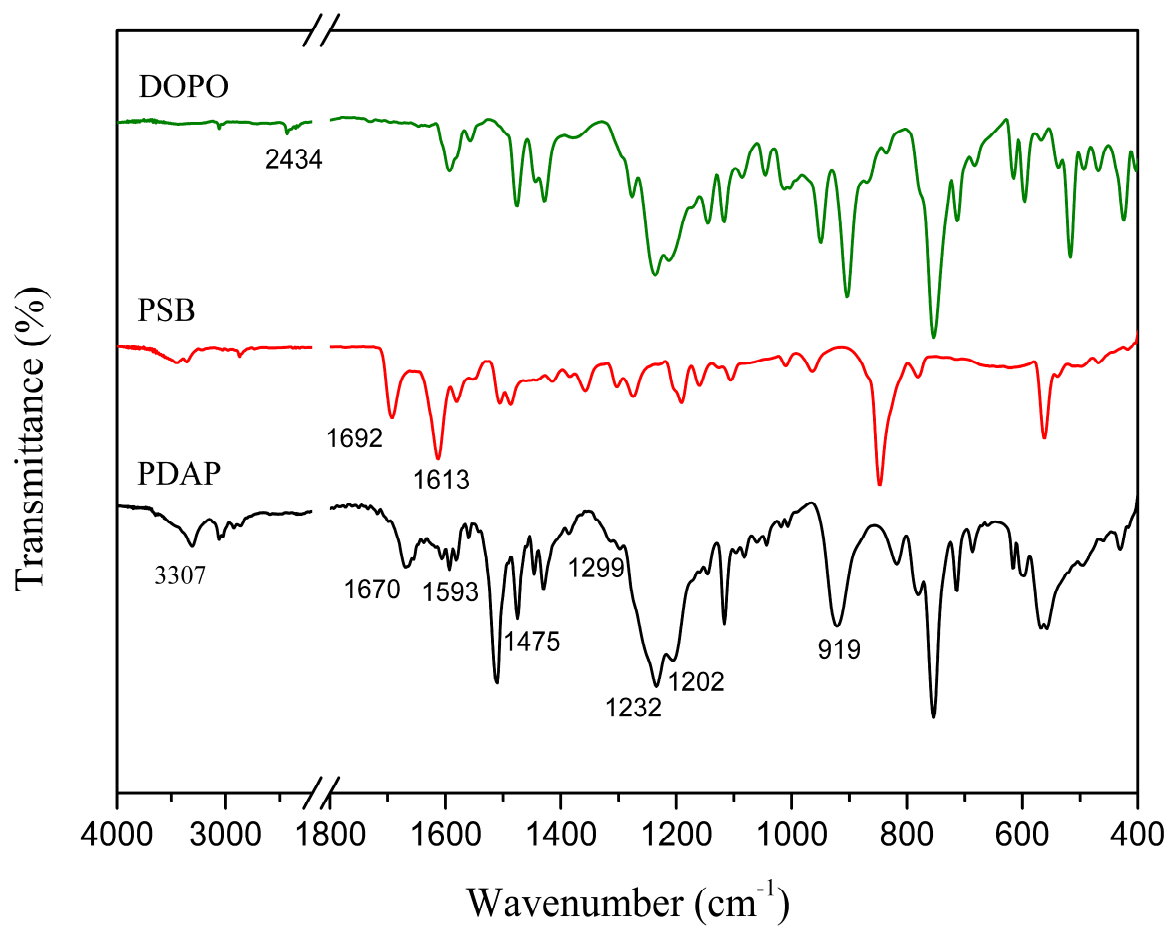
^b BC, burn to clamp.

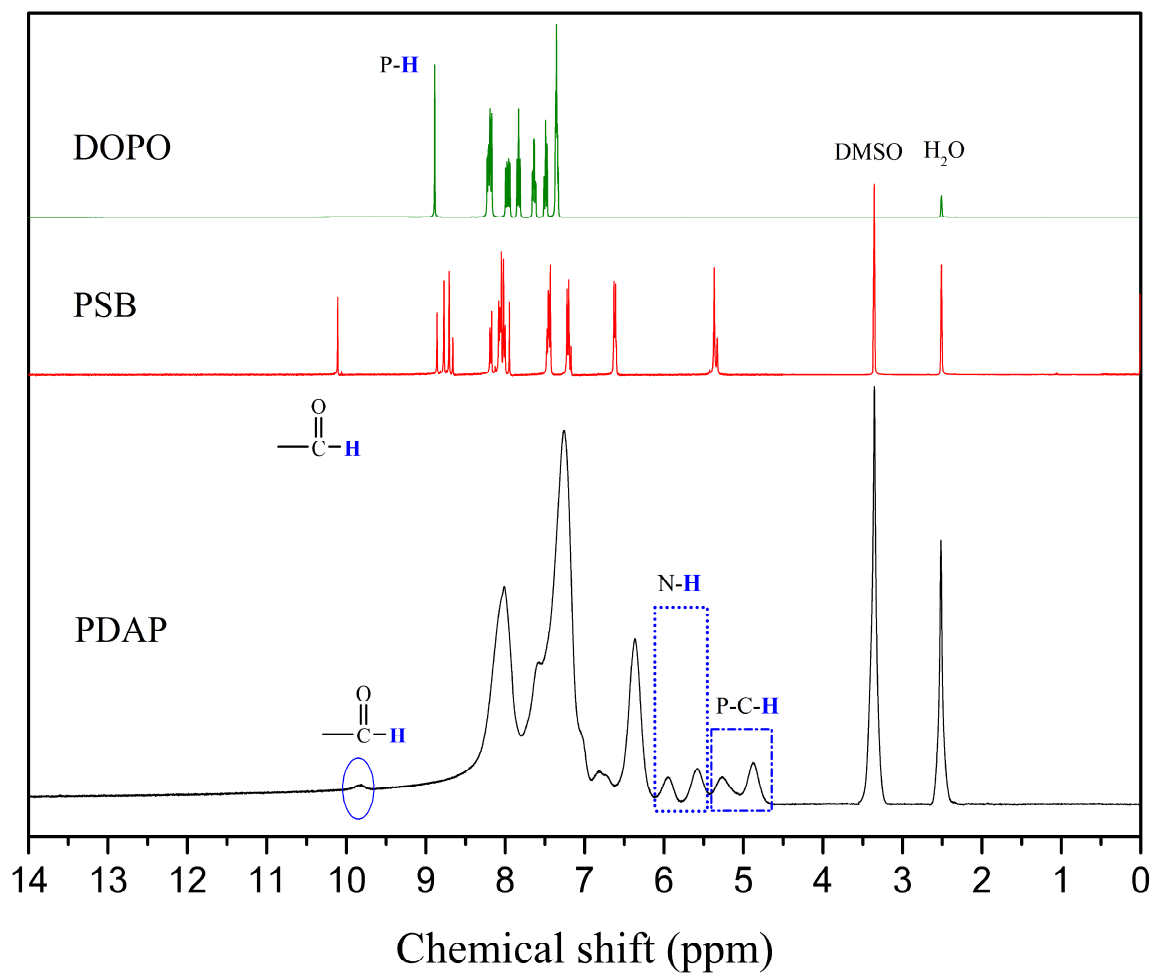
Table 4. Pyrolysis products identified in the pyrograms of EP and EP/PDAP7

No.	m/z	Assigned structure	Relative area (%)	
			EP	EP/PDAP7
a	44		3.68	2.52
b	44		2.47	1.57
c	58		1.12	0.96
d	118		0.61	0.47
e	94		25.27	16.43
f	121		0.96	1.84
g	132		1.42	1.27
h	135		0.98	1.17
i	136		6.99	8.68
j	134		24.51	15.72
k	154		—	1.33
l	168		—	3.32
m	170		—	6.34
n	183		1.64	0.94
o	212		12.27	1.83
p	226		6.31	2.25
q	242		2.25	1.36
r	228		0.47	17.85
s	252		3.24	5.85
t	240		3.67	5.18
u	254		2.14	3.12

Scheme 1. Synthetic route of PDAP







ACCEPTED

